

Use of Amorphous Silicon (ASi) Electronic Portal Imaging Devices for Other applications for Linear Accelerator Quality Assurance

Gena Mohamed¹, Khalid. M. El-Shahat², Mahmoud Salem³, Atef. El-Taher^{4*}

1. Assiut Military Center for Radiotherapy, Assiut, Egypt
2. Faculty of Medicine, Al Azhar University, Egypt
3. Physics Department, Faculty of Science, New Valley University, 72511, El-Kharga, Egypt.
4. Physics Department, Faculty of Science, Al Azhar University, Assuit

ARTICLE INFO	ABSTRACT
<p>Article type: Original Paper</p> <hr/> <p>Article history: Received: Dec 29, 2019 Accepted: May 14, 2020</p> <hr/> <p>Keywords: Portal Imaging Dosimetric Properties Electronic Portal Imaging Devices (EPID) Radiation Dosimetry</p>	<p>Introduction: The success of radiation therapy depends critically on the accuracy of patient alignment in treatment position day after day. The primary use for Electronic portal imaging devices (EPIDs) is to monitor patient position during daily radiotherapy sessions. Recently the role of EPIDs has been expanded beyond patient imaging to become a useful tool for radiotherapy dosimetry.</p> <p>Material and Methods: To test another application of linac quality assurance (QA), 10×10 cm² and 18×18 cm² images of an open field were obtained. The epidermis was located at a fixed detector distance of 150 cm.</p> <p>Results: Wedge profile and wedge factors with a high level of accuracy demonstrated. The profiles acquired using EPID deviated in shape and magnitude by up to 16% from the ion chamber profiles. The use of EPID for linac QA can be simplified by improving the available software analysis tools, which will increase its efficiency. According to the findings, the EPID aSi500 has the potential to be used as a relative dosimeter, making it a straightforward and efficient tool for daily QA.</p> <p>Conclusion: All EPID measurements were performed using the linear accelerator Varian DMX. Based on the physical characteristics, as an efficient tool, the SLIC-EPID can be used for daily QA.</p>
<p>► Please cite this article as: Mohamed G, El-Shahat Kh, Salem M, El-Taher A. Use of Amorphous Silicon (ASi) Electronic Portal Imaging Devices for Other applications for Linear Accelerator Quality Assurance. Iran J Med Phys 2021; 18: 285-292. 10.22038/ijmp.2020.45434.1701.</p>	

Introduction

Radiation therapy is an essential treatment modality for cancer patients. Its success depends critically on the accuracy of patient alignment in treatment positions day after day. The introduction of the electronic portal imaging device (EPID) has been a great step towards overcoming the issues with conventional film dosimetry and 2D detector array [1]. Electronic portal imaging devices (EPIDs) are widely used to monitor patient position during daily radiotherapy sessions. Several online and offline verification protocols have been developed for this purpose [2-3]. Portal images are usually taken to verify patient set-up and positioning before radiation therapy treatment. With excellent dosimetric characteristics, EPID has been expanded to patient dosimetry measurements and machine QA during the past decades. Several studies have investigated the use of EPID for QA of virtually every aspect of linac performance, and it has been recently used for all EPID daily QAs [4].

The current study aimed to discover other applications of EPID for linac QA. All available QA tests were considered as an indirect measure of the

dosimetric properties of the linac. The efficiency of QA tests can be increased by using other methods than currently available ones, using an electronic portal imaging device (EPID).

Materials and Methods

Linear accelerator Varian DMX with Amorphous Silicon (aSi) 500 EPID was used for all measurements. Linear accelerator Varian DMX can produce 6 MV and 15 MV photon beam with a wide range of dose rates, ranging from 100 to 600 MU/min. Image acquisition was performed with one monitor unit corresponding to a calibrated dose delivery of 1 cGy (1 rad) under the reference conditions (SSD = 100cm, with a 10 × 10 cm² field at a depth of d_{max}) and using available repetition modes (100MU/min) [2-5].

Electronic portal imaging device (EPID)

The Varian amorphous silicon (aSi) EPID was used to verify patients' set-up. The EPID system consists of an image detection unit (IDU) featuring a detector and accessory electronics, an image acquisition system (IAS2) containing acquisition electronics for the IDU

and interfacing hardware, and a dedicated workstation for off-line image review [6-8]. By activating the pixels row after row, an image of almost 200,000 pixels was obtained. Its active detector area is $30 \times 30 \text{ cm}^2$ at SSD 100 cm. The sensitive area, at 150 cm source-detector distance (SDD), was $22 \times 18 \text{ cm}^2$. The scintillator converts the incoming X-rays into visible photons. The light is sensed by a photodiode array attached to the amorphous -silicon panel. Photodiodes integrated the incoming light into charge captures, and the charges transfer from pixels to read-out electronics by the detector electronics.

Phantom studies

The acrylic slab phantom is a phantom used for calibration and depth dose measurements in radiation therapy. The phantom is designed for a range of 70 kV to 50 MV photon radiations and 1 MeV to 50 MeV electron radiations. The phantom consists of 33 acrylic plates with dimensions of $30 \text{ cm} \times 30 \text{ cm}$ [9].

Irregular fields

This test aims to investigate the MLC position around the central axis. So for each MLC pair are needed to measure the distance between the central axis and 50% on the profile, comparing the distance for both MLC pair (Right and Left), and, eventually, calculating the mean difference.

For irregular field profiles, we used a circle shape for a field size of $10 \times 10 \text{ cm}^2$. To make a circular shape, Multileaf Collimator (MLC) was applied to make a circular phantom in TPS. Then, we used EPID to take an image for this phantom, at SED = 150 cm (Figure 1(b)).

The shape was chosen because of its clinical similarity to the Antero-posterior pelvic radiation fields used in the treatment of prostate cancer (Figure 1(a)). The image was then reviewed and analyzed. The profiles were investigated.

Verification of radiation isocenter

The radiation isocenter of the linac should be verified routinely, using collimator and gantry rotation about a sphere of 1mm radius. This test is conventionally performed with the use of films.

Collimator spoke shot

QA patient was set-up in TPS, a plan was created with the upper jaws opened to 40 cm, and the lower collimator jaws were closed to give a slit of 0.5 cm width symmetrically. Images were acquired with collimator angles 0, 30, 60, 120, 270, & 330 (Figure 2). These images were then reviewed and analyzed in the dosimetry workspace under Review Task. The images of EPID with collimator rotation should be combined or added together to make a sphere to analyze it and calculating its radius.

Using the phantom has the advantage of providing an accurate estimation of the distance between two points on the image. The center of each image can be found using the measure tool and a line drawn to pass through the center. This process was iterate for the image of every collimator angle, which forms a triangle in the center. Then, the length of the longest side of the triangle and correspondingly the diameter of the circle within it can be measured.

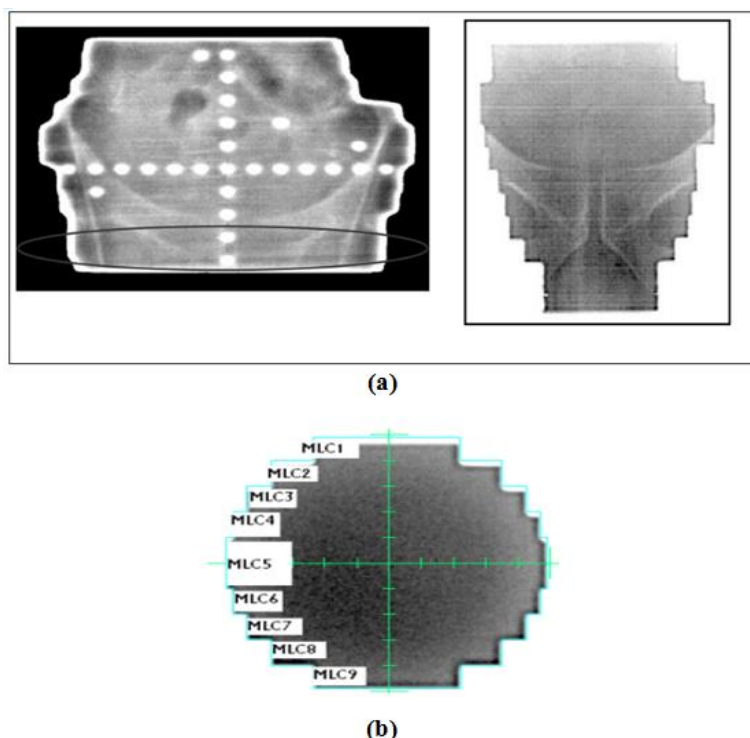


Figure 1. a) Anterior-posterior pelvic radiation fields [8], b) Image of EPID for circular shape for field size $10 \times 10 \text{ cm}^2$.

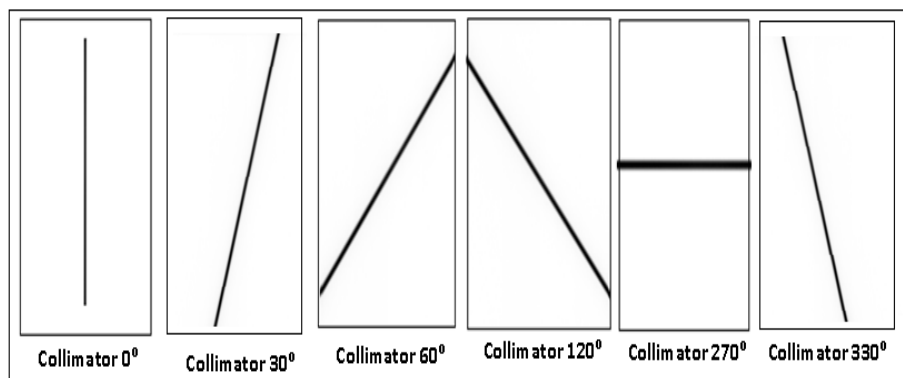


Figure 2. Collimator rotation images with different collimator angles of 0°,30°,60°, 120°, 270°, and 330°

Wedge angle

Wedge angles, known as the angle between the 50% isodose contour and the perpendicular to the central beam axis, ranged from 10° to 60°. The heel was defined as the thick end of the wedge, which had the lowest dose, while the thin edge of the wedge is named the toe (Figure 3).

The wedge profiles measured by EPID from the open and wedge field images acquired at SED = 100 cm for a field size of 10×10cm² and 18×18cm² were compared to the wedge profiles measured with semi-flex at SDD =100 cm, and wedge angles of 30°, 45°, and 60°. It worth noting that the wedge 15° was omitted because of a problem.

Wedge factor

The wedge factor was used to monitor unit calculations to recompense the reduction in beam transmission produced by the wedge. The wedge factor is known as the proportion of doses at Z_{max} in a water phantom on the central beam axis (point P) both with and without the wedge. The wedge factor mainly relies on the depth and size of the field [11].

The wedge factors measured using EPID from the open and wedge field images acquired at SED = 100 cm for a field size of 10 × 10 cm² were compared with semi-flex at SDD =100 cm wedge angles of 30°, 45°, and 60°. The next figure shows the images of EPID both before and after wedge (Figure 4). It clearly shows the

effect of the wedge on the pixels. There is a gradient in the resolution of an image. The pixel value of the center of each image can be found using the pixel Information tool.

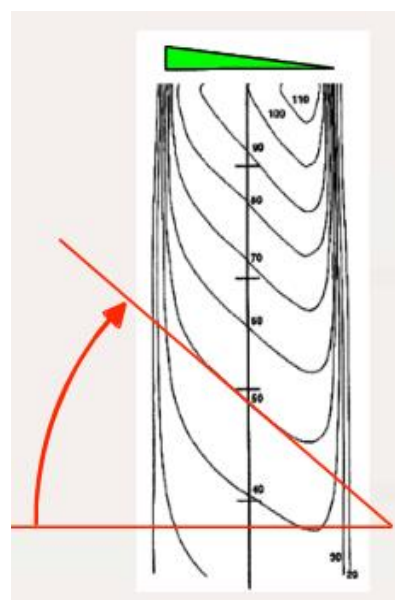


Figure 3. Wedge angle measured in the isodose curve [9]

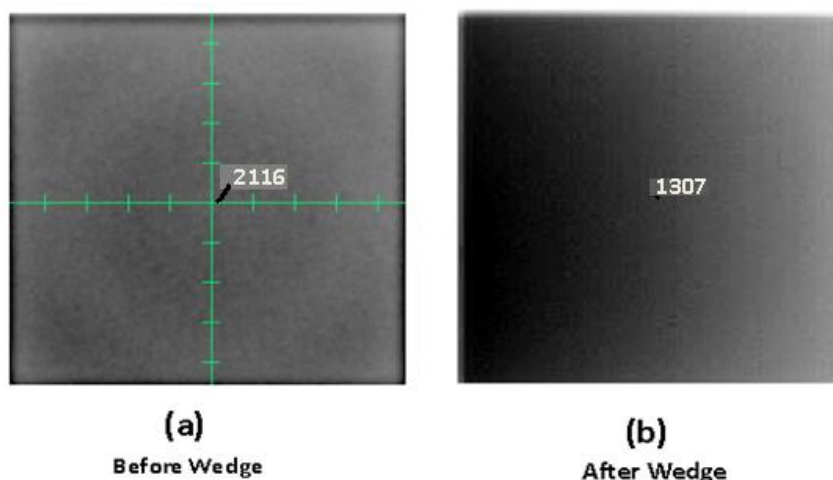


Figure 4. Images of EPID of the field size 10×10 cm²: (a) Before wedge; and (b) After wedge 30°.

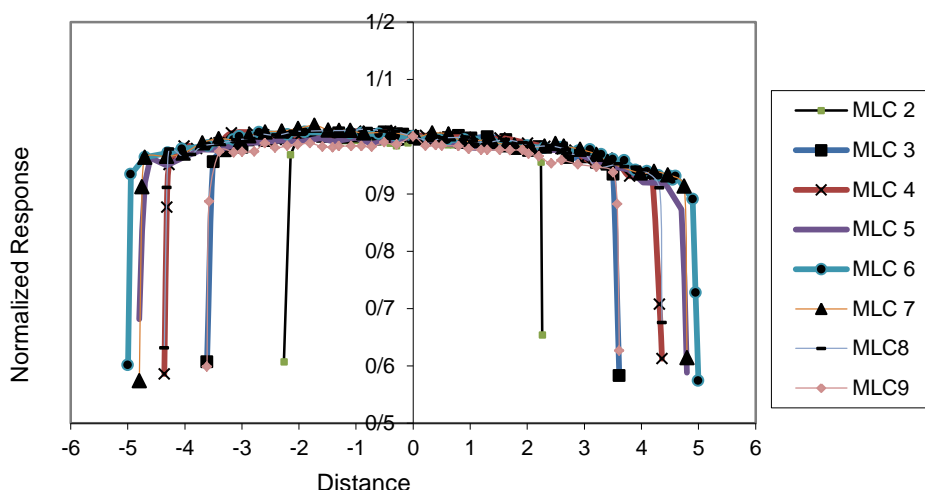


Figure 5. Line profiles of circular shape for the field size of 10×10 cm² at each MLC.

Results

Irregular field profiles

In the present study, the MLC position around the central axis was investigated. For each MLC pair, we measured the distance between the central axis and the 50% on the profile. In addition, the distance for both MLC pair (Right and Left) was compared, following by calculating the mean difference.

Images with EPID at SED = 150 cm were taken for a circular field size of 10×10 cm². The line profiles of circular shape for a field size of 10×10 cm² at each MLC were so closed (Figure 5), the results were normalized. For each MLC pair, the distance between the central axis and 50% on the profile was measured, and the distance between both MLC pair (Right and Left) was compared [12], and, eventually, the mean distance difference between the MLC pair was found 0.01 cm, which indicates a good movement of MLC pair.

Verification of radiation isocenter

By using local phantoms, which were applied for routine pretreatment QA, the radiation isocenter was verified [13], which was performed with a collimator about a sphere of 1mm radius.

Collimator spoke shot

Images with collimator angles of 0, 30, 60, 120, 270, & 330° were taken at SSD 150 cm and a field size of 0.5×40 cm². The images of EPID with collimator rotation were combined or added together to make a sphere according to the American Association of Physicists in Medicine (AAPM) REPORT NO. 72 protocols. The resultant combined images were scaled for distance.

Using the phantom has the advantage of giving an accurate distance between two points on the image. The centre of each image can be found using the measure tool and a line drawn to pass through the centre. This is

repeated for the image of every collimator angle, which forms a circle in the centre as shown in figures 6, 7. The diameter of the circle is measured. We found that the radius is 0.2 mm, which is within tolerance ≤ 1 mm. That shows that it is feasible to use EPID for Collimator spoke shot test.

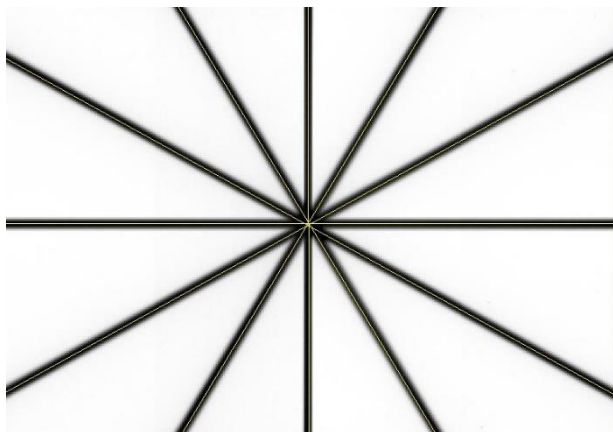


Figure 6. Collimator rotation "combined" resultant image.

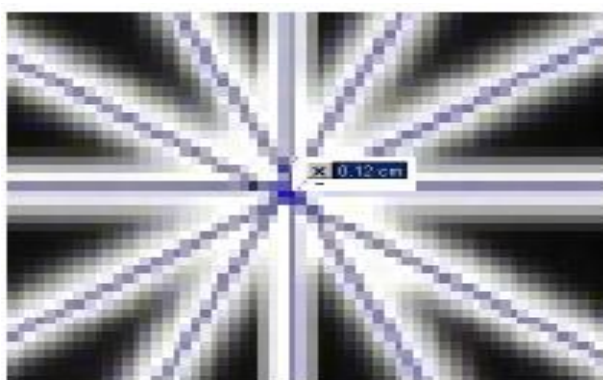


Figure 7. Collimator rotation magnified resultant image

Wedge profile

The radial profiles measured at SDD = 100 cm using semi-flex and SED = 100 cm for EPID. The following figures show a comparison of these radial profiles acquired at SED = 100 cm for different wedge angles and field sizes. The wedged profiles acquired with EPID and chamber without using any buildup material for the flooded field are shown in Figures 8 to 13. For the field size of 10×10 cm², the profiles obtained with EPID showed better standard deviation (3.9%) compared to the chamber (4.8%). For the field size of 18×18 cm², the maximum standard deviations of 4.6% and 5.1% were acquired for EPID and chamber, respectively. For the more extensive field size of 18×18 cm², the profiles acquired using EPID deviated from chamber profiles up to 4% at the 'hot edge' or the high dose region of the wedge profile and to 6% for field size 10×10 cm², which is better than those reported by Jhala, E. (2006) [2]. On the other hand, profiles acquired for the field size of 18×18 cm², using the Varian method of calibration for EPID, deviated from LA48 ion chamber profiles up to 8% at the 'hot edge' of the EDW profile. The wedge profiles exhibited a deviation from the ion chamber in the tails and the penumbra region. It was also found that the maximum difference between any EPID measurement and semi-flex was within 8%. Jhala (2006) reported better results in the shoulders region. The profiles acquired using EPID agree within 1% of LA48 profiles in all regions except for the 'hot edge' of the EDW profiles. In this study, the 'shoulders' of the EPID profiles showed almost a 5 mm discrepancy from the profiles acquired using semi-flex. The EPID profiles seem to be better than the ion chamber profiles, which also showed unacceptable distortion [2].

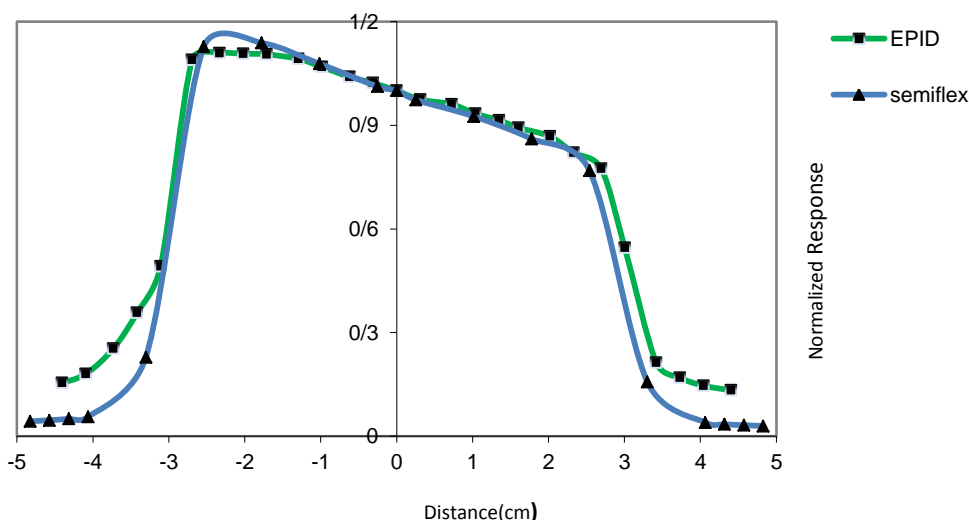


Figure 8. Comparison of 10×10 cm² wedge of 60° profiles acquired using semi-flex & EPID without buildup for flood field

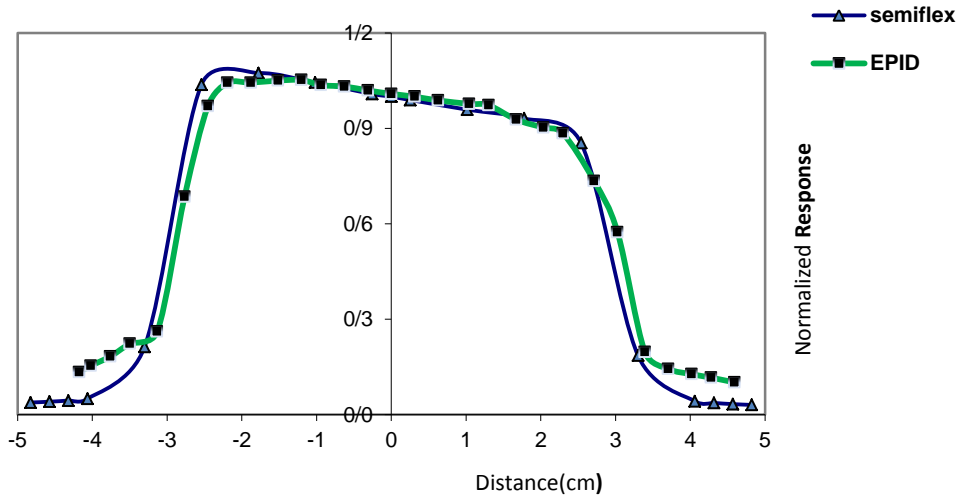


Figure 9. Comparison of $10 \times 10 \text{ cm}^2$ wedge of 45° profiles acquired using semi-flex & EPID without buildup for flood field

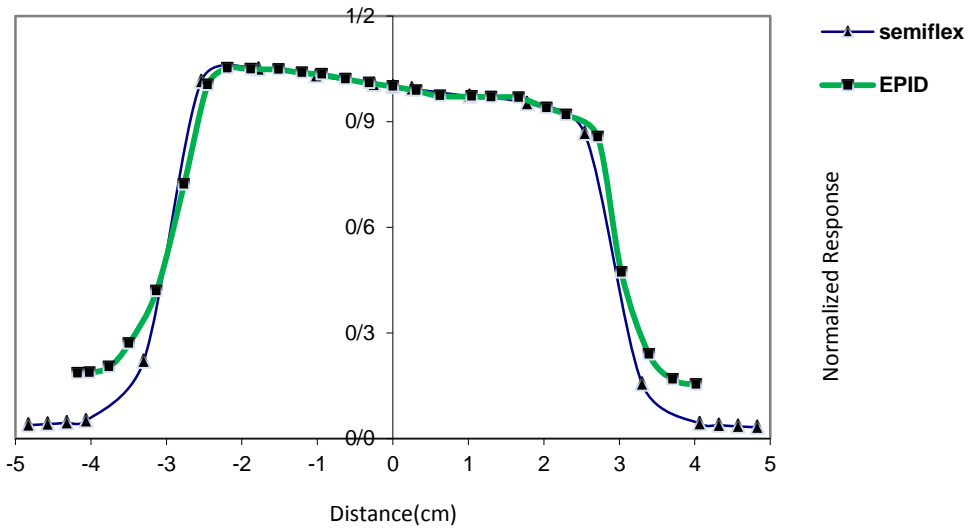


Figure 10. Comparison of $10 \times 10 \text{ cm}^2$ wedge of 30° profiles acquired using semi-flex & EPID without buildup for flood field.

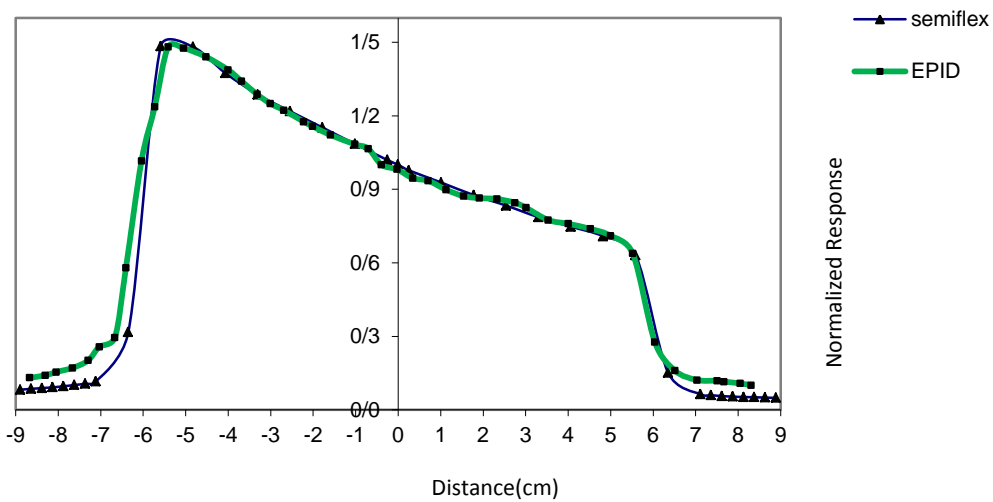


Figure 11. Comparison of $18 \times 18 \text{ cm}^2$ wedge of 60° profiles acquired using semi flex & EPID without buildup for flood field

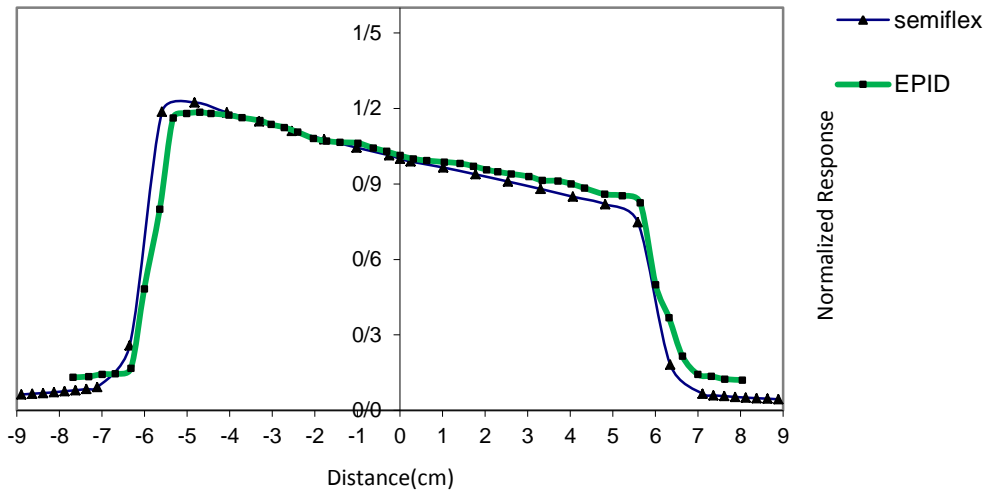


Figure 12. Comparison of 18x18 cm² wedge of 45° profiles acquired using semi-flex & EPID without buildup for flood field

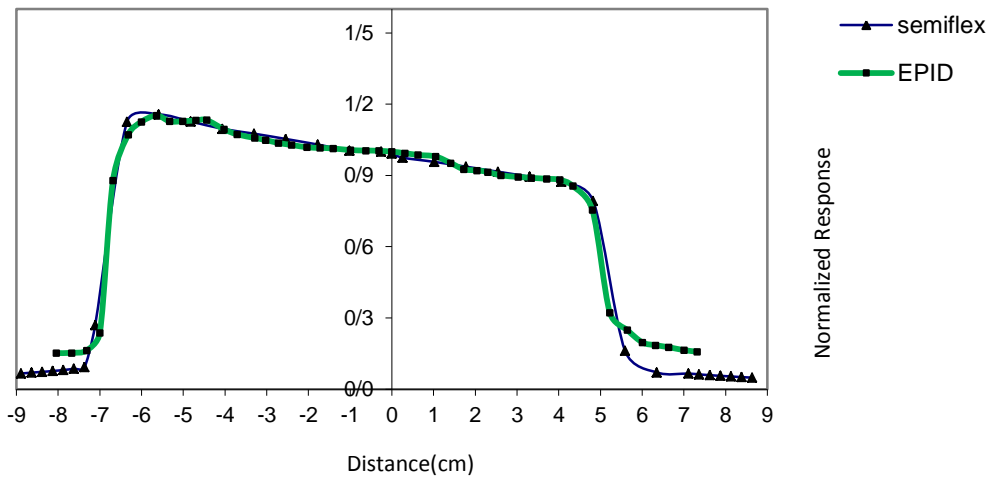


Figure 13. Comparison of 18 x 18 cm² wedge of 30° profiles acquired using semi-flex & EPID without buildup for flood field

Table1. Comparison between wedge factors measured by EPID for the field size of 10 x 10 cm² and wedge factors measured with the ion chamber.

Wedge degree	Reading chamber (nC)	for	Reading for EPID (Pixel value)	Wedge factor for chamber	Wedge factor by EPID	WF(EPID) / WF (chamber) x 100
Open field	95.63		2116	-----	-----	-----
30	58.946		1307	0.6164	0.6177	1.002
45	46.21		1019	0.4832	0.4816	0.997
60	37.64		797	0.3936	0.3767	0.96

Wedge factor

The wedge factors (WF) for the field size of 10 x 10 cm² were compared to the wedge factors measured with ion chamber semi-flex at SSD = 100 cm for the field size of 10 x 10 cm. The pixel value of the center of each image can be determined using the pixel Information tool. The measured wedge factors for ionization chamber and EPID are provided in Table 1 [2].

In wedge 30, the wedge factor measured by chamber was 0.6164, while the wedge factor measured by EPID

was 0.6177. By dividing 0.6177 on 0.6164, a value of 1.002 was obtained. By iterating a similar process for wedges 45 and 60, the resultant wedge factors measured by EPID were found to be within 1% of the wedge factors measured by the ion chamber. In the same vein, Gibbons reported a similar range of 1% [14]. The wedge factor is a ratio of open field and wedged field; hence, it can cancel any effect from extended SSD, which is in line with the agreement within 1% of the calculated factors. Hence, it can be argued that the EPID can be

used to measure the wedge factors with a high level of accuracy. According to the results, the aS500 EPID has the potential to be used as a relative dosimeter, which made it a straightforward and efficient tool for daily QA.

Discussion

This study demonstrated EPID can be used as a standard physics tool for linear accelerator QA. By taking images with collimator angles of 0, 30, 60, 120, 270, & 330 ° at SSD150 cm and a field size of 0.5×40 cm², the radius was 0.2 mm, which is within the tolerance of ≤1 mm. Collimator spoke shot test was successful.

The radiation isocenter of the linac was verified, which was performed with collimator rotation about a sphere of 1 mm radius. In addition, the radius was 0.2 mm, which is within the tolerance of ≤1 mm. The MLC position around the central axis was found 0.01 cm, which indicates the good movement of the MLC pair. The wedge factors measured by EPID were found to be within 1% of the wedge factors measured by the ion chamber. They were also found to be within 1% of the theoretically calculated wedge factors illustrated by a study performed by Gibbons [15].

Conclusion

The main objective of Electronic Portal Imaging Devices (EPIDs) development has been positioning verification. Nevertheless, in the present study, we applied EPID for QA purposes. According to the findings, all aSi EPID measurements were performed at an SDD of 150 cm.

At small heights, more scattered photons fell on the EPID, which resulted in decreased accuracy of the dosimetric calibration procedure. At 160 cm, less scattered photons reached the EPID; however, the maximum field of view (FOV) was decreased; In the present study, a height of 150 cm was chosen as the tradeoff between FOV and dosimetric accuracy. No saturation effect was noticed in the profiles measured at SDD = 150 cm, which indicated the good agreement with ion chamber profiles. According to the findings, the aS500 EPID has the potential to be used as a relative dosimeter; making it a straightforward and efficient tool for daily QA.

References

- Gandhi A, Vellaiyan S, Subramanian VS, Shanmugam T, Murugesan K, Subramanian K. Commissioning of portal dosimetry using a novel method for flattening filter-free photon beam in a nontrue beam linear accelerator. *Journal of cancer research and therapeutics*. 2019 Jan 1;15(1):223.
- Jhala E. Investigation of Dosimetric Characteristics and Exploration of Potential Applications of Amorphous Silicon Detector. 2006.
- Langmack KA. Portal imaging. *The British journal of radiology*. 2001 Sep;74(885):789-804.
- Sun B, Goddu SM, Mutic S, Cai B. EPID-based linear accelerator benchmarking using pixel sensitivity map. *InJournal of Physics: Conference Series* 2019 Aug 1; 1305(1):012063.
- Gena MA, El-Attar AL, Zahran EM, El-Gamal H, Aly MM. Development of the Use of Amorphous Silicon (ASi) Electronic Portal Imaging Devices as a Physics Tool for Routine Linear Accelerator QA.
- Liu G. The Application of Electronic Portal Imaging Devices to Radiotherapy Quality Assurance (Doctoral dissertation, University of Adelaide. 2002).
- Kavuma A. Transit dosimetry based on water equivalent path length measured with an amorphous silicon electronic portal imaging device (Doctoral dissertation, University of Glasgow). 2011.
- De Koste JR, Cuijpers JP, de Geest FG, Lagerwaard FJ, Slotman BJ, Senan S. Verifying 4D gated radiotherapy using time-integrated electronic portal imaging: a phantom and clinical study. *Radiation Oncology*. 2007 Dec;2(1):1-9.
- Lloyd PJ. Quality assurance workbook for radiographers and radiological technologists. World Health Organization. 2001.
- Kirby MC, Glendinning AG. Developments in electronic portal imaging systems. *The British journal of radiology*. 2006 Sep;79(special_issue_1):S50-65.
- Giraud P, De Rycke Y, Rosenwald JC, Cosset JM. Conformal radiotherapy planning for lung cancer: analysis of set-up uncertainties. *Cancer investigation*. 2007 Jan 1;25(1):38-46.
- Pasler M, Hernandez V, Jornet N, Clark CH. Novel methodologies for dosimetry audits: Adapting to advanced radiotherapy techniques. *Physics and Imaging in Radiation Oncology*. 2018 Jan 1;5:76-84.
- Gibbons JP. Calculation of enhanced dynamic wedge factors for symmetric and asymmetric photon fields. *Medical physics*. 1998 Aug;25(8):1411-8.
- Jacobs M, Nijsten SM, Lambin P, Minken AW. 6 Dosimetric calibration of a Siemens OptiVue 500 amorphous silicon electronic portal imaging device. *Radiotherapy and Oncology*. 2005(76):S15-6.